Energy Dependent Tunneling in a Quantum Dot

K. MacLean,[1] S. Amasha,[1] Iuliana P. Radu,[1] D. M. Zumbühl,[1,2] M. A. Kastner,[1] M. P. Hanson,[3] and A. C. Gossard[3]

[1]Department of Physics, Massachusetts Institute of Technology, Cambridge, Massachusetts 02139
[2]Department of Physics and Astronomy, University of Basel, Klingelbergstrasse 82, 4056 Basel, Switzerland
[3]Materials Department, University of California, Santa Barbara 93106-5050

We present measurements of the rates for an electron to tunnel on and off a quantum dot, obtained using a quantum point contact charge sensor. The tunnel rates show exponential dependence on drain-source bias and plunger gate voltages. The tunneling process is shown to be elastic, and a model describing tunneling in terms of the dot energy relative to the height of the tunnel barrier quantitatively describes the measurements.

PACS numbers: 73.43.Jn, 73.63.Kv, 73.23.Hk

Gate controlled quantum dots have been used to study a wide variety of physical phenomena, from correlated-electron physics [1], which becomes important when the coupling of the dot to its leads is strong, to the coherence of electron charge and spin states [2], which can be maintained only when the coupling to the leads is weak. Observation of these phenomena is made possible by in-situ control of the rate of tunneling , coupling the dot to its leads: can be adjusted over more than ten orders of magnitude by changing the voltages applied to the gates that define the tunnel barriers of the quantum dot. Recently, integrated charge sensors [3] have made possible a variety of new investigations of , probing the effect of excited states [4, 5, 6], electron number [7], barrier symmetry [8, 9] and Coulomb interactions [9, 10].

In this Letter, we report exponential sensitivity of the rates for electrons tunneling on ($_{on}$) and off ($_{off}$) a lateral GaAs quantum dot as a function of the drain-source bias V_{ds} and plunger gate voltage V_g. The tunnel rates are obtained by performing time resolved measurements of a quantum point contact (QPC) charge sensor adjacent to the dot [11, 12, 13] and utilizing pulsed-gate techniques [11, 14]. We show that the tunneling is dominated by elastic processes, and that the measured exponential dependence of on V_{ds} and V_g is in excellent quantitative agreement with a model describing tunneling in terms of the dot energy relative to the height of the tunnel barrier.

The device used in this work is fabricated from a AlGaAs/GaAs heterostructure grown by molecular beam epitaxy. The two dimensional electron gas (2DEG) formed at the AlGaAs/GaAs interface 110 nm below the surface of the heterostructure has a mobility of 6.4 10^5 cm^2/Vs and density of 2.2 10^{11} cm^{-2} [17]. An electron micrograph of the gate geometry is shown in Fig. 1 (a) and is similar to that of Ciorga et al. [18]. Applying negative voltages to the labeled gates forms a single dot containing one electron coupled to the surrounding 2DEG through two tunnel barriers: One between SG1 and OG (b1, connecting the dot to lead 1) and the other between SG2 and OG (b2, connecting the dot to lead 2). Lead 2 is grounded, and a voltage V_{ds} is applied to lead 1. Approximately the same DC voltage V_g is applied to the three plunger gates LP1, PL, and LP2. We have verified that a single, not double, dot is formed. We measure the dot in a dilution refrigerator with a lowest electron temperature of 120 mK.

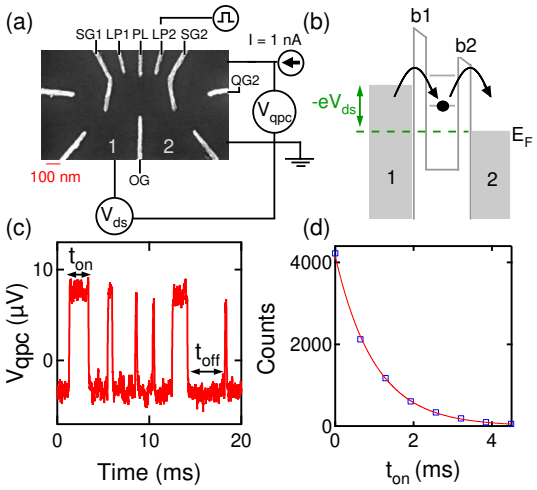

FIG. 1: (a) Electron micrograph of the gate geometry and schematic of the measurement circuit. Unlabeled gates are grounded. We measure the resistance of the QPC by sourcing a current through the QPC and monitoring the voltage V_{qpc} across the QPC. We have verified that the finite bandwidth of our measurement [15] does not significantly affect the results presented in this work using computer simulations. (b) When a voltage bias V_{ds} is applied across the quantum dot a small current flows and the charge on the dot fluctuates between 0 and 1 as shown in (c). We measure the time intervals t_{on} (t_{off}) that the electron is on (off) the dot using an automated triggering and acquisition system described in Ref. [16]. The offset in the trace is caused by the AC coupling of the voltage preamplifier. (d) Histogram of t_{on} times from data such as in (c). Fitting this histogram yields $_{off}$ as described in the text.

Applying a negative voltage to the gate QG2, we form a QPC between the gates QG2 and SG2. The resistance of the QPC is sensitive to the charge on the dot [3], allowing us to measure the number of electrons on the dot in real time [11, 12, 13]. If we apply a drain-source bias

V_{ds} across the dot (Fig. 1(b)), we observe the number of electrons on the dot fluctuate between 0 and 1. A typical trace is shown in Fig. 1(c). To measure Γ_{off}, we histogram the times t_{on} that the electron spends on the dot (Fig. 1(d)) and fit to an exponential $A e^{-\Gamma_{off} t_{on}}$ [13]. We obtain Γ_{on} from the time intervals t_{off} in the same manner. Using this technique we measure Γ_{off} and Γ_{on} as a function of V_{ds} (Fig. 2(a)) for the case in which there is either 0 or 1 electrons on the dot at the position shown in Fig. 2(b). As V_{ds} is made more negative, Γ_{off} is seen to increase exponentially.

To model the tunneling rates, we linearize the exponential in the WKB formula for tunneling through a barrier [19] for a small perturbation E to the dot energy E and a small deviation U of the tunnel barrier potential $U(x)$: $\Gamma = \Gamma_0 \exp[-(U - E)]$, where Γ and Γ_0 depend on the details of the barrier potential. In a simple capacitor model for the dot we assume a linear dependence of E on small perturbations V_g and V_{ds} about arbitrary but fixed V_{ds} and V_g values: $E = -e\alpha_{dsE} V_{ds} - e\alpha_{gE} V_g$, where α_{dsE} is the ratio of the drain-source capacitance to the total dot capacitance, and α_{gE} is the capacitance ratio for the three plunger gates. Similarly, U varies linearly as $U = -e\alpha_{dsU} V_{ds} - e\alpha_{gU} V_g$, where α_{dsU} and α_{gU} give the coupling of V_{ds} and V_g to the barrier potential. There will, of course, be different parameters α_{dsU}, α_{gU}, and Γ_0 for the two barriers. Note that Γ depends exponentially on $U - E$, and therefore depends exponentially on V_{ds} and V_g: One can show that this holds independent of the particular shape $U(x)$ of the barrier potential, or the shape of the perturbation to the potential induced by the change V_g or V_{ds}. Using this linearization, we can write down equations for the V_{ds} dependence of Γ_{off} and Γ_{on}, including Fermi statistics in the leads, assuming elastic tunneling, and considering only a single orbital state of the dot:

$$\Gamma_{off} = \Gamma_{2;0} e^{-\alpha_2 V_{ds}} (1 - f_2(E)) + \Gamma_{1;0} e^{-\alpha_1 V_{ds}} (1 - f_1(E)) \quad (1)$$

$$\Gamma_{on} = \Gamma_{2;0} e^{-\alpha_2 V_{ds}} f_2(E) + \Gamma_{1;0} e^{-\alpha_1 V_{ds}} f_1(E) \quad (2)$$

Here $\alpha_{1;2} = \alpha_{1;2} / |\alpha_{dsU_{1;2}} - \alpha_{dsE}|$, $E = -e\alpha_{dsE} V_{ds} - e\alpha_{gE} V_g$ is the energy of the one-electron state relative to the Fermi energy E_F, and αV_g is the shift in V_g from the 0 to 1 electron transition. f_2 and f_1 are the Fermi functions of the two leads $f_2(E) = f(E)$, $f_1(E) = f(E + eV_{ds})$, and Γ is the ratio between the tunnel rate onto and off of the dot for a given lead when the one-electron state is aligned with the Fermi level in that lead. We expect that $\Gamma = 2$ because of spin degeneracy [10, 20], and use this value in the calculations below.

To understand Fig. 2(a), we note that whether Γ_{on} increases or decreases with V_{ds} depends on whether lead 1 is better coupled to the barrier or the dot, that is, whether α_{dsU} or α_{dsE} is larger. Since b1 is closer to lead 1 than the dot, and b2 is farther from lead 1 than the dot, it follows that $\alpha_{dsU_1} > \alpha_{dsE} > \alpha_{dsU_2}$ (see Fig. 1(b)) [21]. Therefore, tunneling through b1 (b2) increases (decreases) exponentially with increasing V_{ds}. This is reflected in the signs of the exponentials appearing in Eq. 1 and Eq. 2.

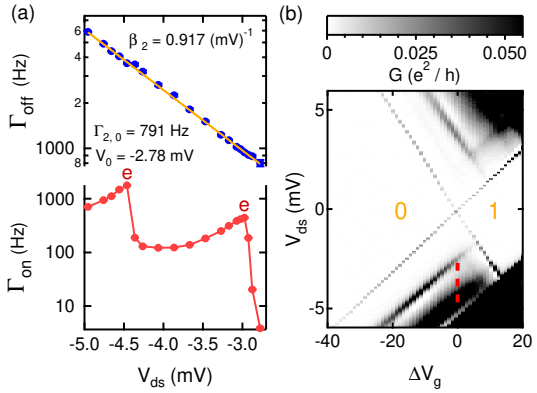

FIG. 2: (a). Γ_{on} and Γ_{off} as a function of V_{ds} for large negative V_{ds}. The solid line in the upper panel is based on a theoretical fit to the data discussed in the text. (b). Differential conductance vs. V_{ds} and V_g, showing the 0 to 1 electron transition. The tunnel rates for this case are made large enough so that the differential conductance can be measured using standard transport techniques. The data shown in (a) are taken at the position of the dashed line.

The solid line through the the Γ_{off} data in Fig. 2(a) is a fit to Eq. 1, which for large negative bias reduces to $\Gamma_{2;0} e^{-\alpha_2 V_{ds}}$. The rate Γ_{on} is shown as a function of V_{ds} in the lower panel of Fig. 2(a). At the two points marked "e" in the figure Γ_{on} increases rapidly as the Fermi energy in lead 1 is aligned with an excited orbital state of the dot [6], giving the 1st and 2nd excited state energies to be 1.9 and 2.9 meV, respectively, above the ground state. The higher-energy states are better coupled to the leads and thus Γ_{on} rises rapidly when these states become available. These energies can also be measured, with larger tunneling rates through b1 and b2, using standard transport techniques [22] (Fig. 2(b)), and the results are consistent. We note that Γ_{off} does not show any special features at these points: This is because the electron decays rapidly out of the excited orbital states and subsequently tunnels off the dot from the ground state [6]. We therefore continue to use Eq. 1 when there are multiple orbital states in the transport window.

In the regions between the points marked "e", Γ_{on} is seen to decrease exponentially as V_{ds} is made more negative, as expected from Eq. 2. Note that this decrease in Γ_{on}, with increasingly negative V_{ds}, occurs even though the number of electrons that could tunnel onto the dot inelastically from lead 1 is growing, presenting strong evidence that the tunneling is predominantly elastic, domi-

nated by states very close to the dot energy E . There is, however, an apparent attening of $_{on}$ above the extrapolated exponential decrease near V_{ds} = -4 mV, close to the second excited orbital state. We nd that this line shape is consistent with broadening of the second excited state by a lorentzian of full-width at half-maximum 10 eV. Calculated line shapes are shown for the broadening of the rst excited state in Fig. 3 and are discussed below.

If a square barrier is assumed, one can compute an e ective barrier height U_2 and width w_2 for b2 from the t in Fig. 2(a). For a square barrier = $f_0 e^{2w_2\sqrt{2m(U_2 E)}/h^2}$ [19]. Linearizing the square root in the exponential and estimating $_{dsE}$ $_{dsU_2}$ $_{dsE}$ and f_0 $E_{'s}/h$ 1 THz, where $E_{'s}$ is the level spacing of the dot, we obtain w_2 130 nm and U_2 E_F 5 meV at $V_{ds} = V_0$. These values are only logarithmically sensitive to f_0 and thus depend very little on our estimate of this parameter. The voltages we apply to the gates to create the tunnel barriers are the same order of magnitude as the voltages at which the 2DEG depletes and thus it is reasonable that U_2 E_F is found to be comparable to the Fermi energy (E_F 7.7 meV). The value for w_2 is also reasonable given the dimensions of our gate pattern and heterostructure.

We next examine, in Fig. 3, the dependence of $_{on}$ and $_{off}$ on V_{ds} for both positive and negative V_{ds}. The data are taken with V_g adjusted so that E is kT away from the 0 to 1 electron transition at V_{ds} = 0. The solid lines in Fig. 3 are calculated from Eq. 1 and Eq. 2 and are in good agreement with the data. We note that the value of $_1$ is very close to the value of $_2$. If the height and width of b1 and b2 are comparable one can show that $_1$ $\frac{dsU_1}{dsE}\frac{dsE}{dsU_2}$ $_2$, and it is therefore expected that $_1$ $_2$.

At V_{ds} 3 mV in Fig. 3, the rst excited orbital state is aligned with the Fermi energy in lead 1. For slightly less negative values of V_{ds}, where the excited state is just above the Fermi energy, $_{on}$ appears enhanced above the solid line calculated from Eq. 2. The dashed line in Fig. 3 includes broadening of the rst excited orbital state by a lorentzian of full-width at half-maximum = 13 eV, corresponding to a lifetime broadening of $_{e1}$ = 50 30 ps. Emission of acoustic phonons can lead to excited state lifetimes 100 ps, but for our device parameters we expect much slower relaxation from this mechanism [14, 23, 24]. $_{on}$ also deviates from the solid curve for V_{ds} > 2 mV: This deviation may be caused by broadening of the rst excited state as well. These deviations could also be caused by inelastic processes, which might begin to contribute signi cantly to $_{on}$ when the electron energy is su ciently far below the Fermi energy.

We now turn to the dependence of the tunnel rates on the plunger gate voltage V_g (see Fig. 4). For these measurements, the barriers are tuned so that the tunneling

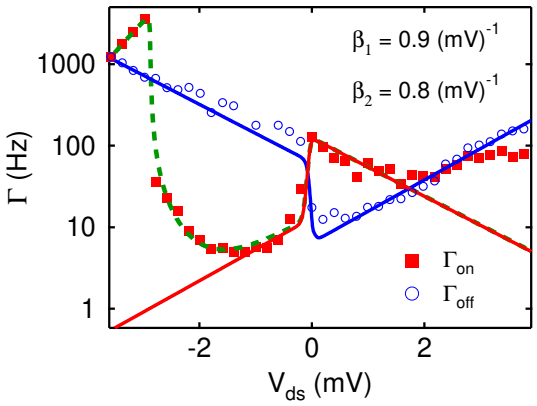

FIG. 3: $_{on}$ (closed squares) and $_{off}$ (open circles) as a function of V_{ds}. The solid and dashed curves are calculations described in the text. The step features near V_{ds} = 0 result from the Fermi distribution.

through b1 is negligible. In the region near V_g = 0 (where E kT), the electron hops on and o the dot spontaneously because there are both electrons and holes in the lead at these energies (Fig. 4(b)). In this region we measure the rates $_{on}$ and $_{off}$ in the same way as described above. In the inset to Fig. 4(a) we compare the probabilities that the electron is on and o the dot p_{on} = $_{on}/(_{on} + _{off})$ and p_{off} = $_{off}/(_{on} + _{off})$ to f(E ;) = $\frac{1}{1+e^{E/kT}}$ and 1 f(E ;), respectively, with T = 120 mK [6].

A pulsed technique (see Fig. 4(c)) is used to measure $_{off}$ when V_g is made su ciently negative that thermally assisted electron tunneling ceases. We begin with the electron energy, determined by V_g, well above E_F. We then apply a positive voltage pulse to the gate LP2 to bring the one-electron energy level near E_F, so that an electron can hop onto the dot. A short time after the pulse the electron will hop o the dot because it is above E_F. We record the time at which this occurs, t, measured relative to the end of the gate pulse. This process is repeated and we make a histogram of the number of tunnel-o events vs. t; an exponential t to this histogram yields $_{off}$. An analogous technique is used to measure $_{on}$ when the one-electron state is well below E_F.

To understand the V_g dependence of , we note that U_2 = $_{gU_2}$ V_g, and $_{gU_2}$ < $_{gE}$ because the three plunger gates are closer to the dot than they are to b2. The dependence of the tunnel rate through b2 on V_g is thus very similar to its dependence on V_{ds} (Fig. 3). Starting at the far left of Fig. 4(a), we see that $_{off}$ decreases exponentially as V_g is made less negative: This is analogous to the $_{off}$ data shown in the top panel of Fig. 2(a) and Fig. 3 (for V_{ds} < 0, where the electron tunnels o through b2). $_{off}$ decreases rapidly at the 0 to 1 electron transition as the ground state is brought below E_F.

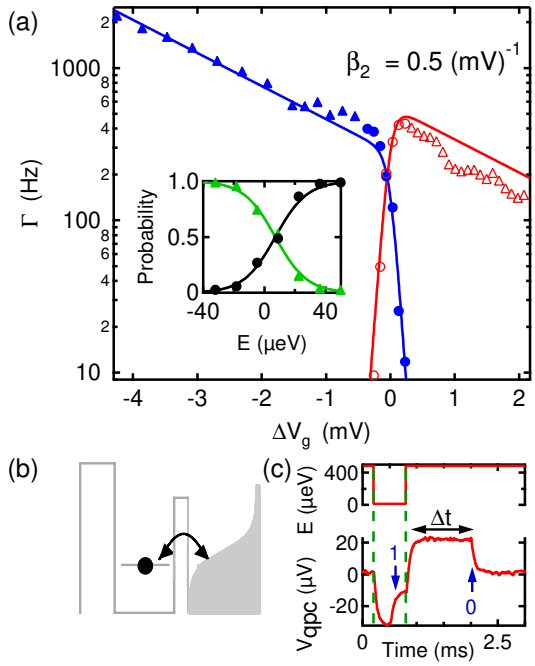

FIG. 4: (a) $_{on}$ and $_{off}$ as a function of V_g. Closed (open) circles are $_{off}$ ($_{on}$) measured by observing spontaneous hopping caused by thermal broadening in the leads as depicted in (b). Closed (open) triangles are $_{off}$ ($_{on}$) measured using a pulsed gate technique. Solid lines are calculations as described in the text. (inset) p_{on} (triangles) and p_{off} (circles) compared to $f(E;)$ and $1 \quad f(E;)$ (solid lines) respectively as described in the text. (b) Sketch of spontaneous hopping caused by thermal broadening in the leads (c) Pulsed technique used to measure $_{off}$. The top panel shows the pulsed modulation of the one-electron state energy E. The bottom panel shows a sample time trace. The dashed vertical lines indicate when the gate pulse begins and ends: The QPC responds to the gate pulse because of direct capacitive coupling to LP2. When the electron energy level is brought near E_F an electron tunnels on the device (indicated by a 1). When the electron level is brought back above E_F the electron tunnels o the device (indicated by a 0).

Continuing into the 1 electron valley we see that $_{on}$ decreases as V_g is made more positive: This is analogous to the $_{on}$ data shown in Fig. 3 (for $V_{ds} > 0$ where the electron tunnels onto the dot through b2). This decrease in $_{on}$ is further evidence that the tunneling is elastic because as the one-electron state is brought farther in energy below E_F there are more electrons that could tunnel onto the dot inelastically at energies closer to the top of the barrier. $_{on}$, however, decreases because elastic tunneling onto the dot happens at a lower energy relative to the barrier height.

We model the data shown in Fig. 4(a) using the same equations as for the drain-source dependence (Eq. 1 and Eq. 2) except with $_{1;0}$ set to zero and V_{ds} replaced by V_g in the exponents. The solid lines in Fig. 4(a) are calculated from Eq. 1 and Eq. 2 with these adjustments and describe the data well. Here again we take = 2, although the t is improved with a smaller value for [10]. We note that the value for $_2$ obtained from the V_g dependence is smaller than the value obtained from the V_{ds} dependence: This is expected because $_{gE} < _{dsE}$.

Summarizing, we nd that the dependence of $_{on}$ and $_{off}$ on V_{ds} and V_g is well described by elastic tunneling at a rate set by the dierence between the electron energy and the barrier height.

We are grateful to J. I. Climente, A. Bertoni, and G. Goldoni for calculations of acoustic phonon emission rates and discussions, to V. N. Golovach, L. Levitov, and D. Loss for discussions, and to I. J. Gelfand, T. Mentzel, V. Rosenhaus, and J. Schirmer for experimental help. This work was supported by the US Army Research Office under Contract W 911NF-05-1-0062, by the National Science Foundation under Grant No. DMR-0353209, and in part by the NSEC Program of the National Science Foundation under Award Number PHY-0117795.

Electronic address: kmaclean@mit.edu

[1] D. Goldhaber-Gordon et al., Nature 391, 156 (1998); S. M. Cronenwett et al., Science 281, 540 (1998).
[2] T. Hayashi et al., Phys. Rev. Lett. 91, 226804 (2003); J. R. Petta et al., Science 309, 2180 (2005); F. H. L. Koppens et al., Nature 442, 766 (2006).
[3] M. Field et al., Phys. Rev. Lett. 70, 1311 (1993).
[4] J. M. Elzerman et al., Appl. Phys. Lett 84, 4617 (2004).
[5] A. C. Johnson et al., Phys. Rev. B 71, 115333 (2005).
[6] S. Gustavsson et al., (2006), cond-mat/0605365.
[7] J. Cooper et al., Physica E 6, 457 (2000); J. Martorell et al., Phys. Rev. B 63, 045325 (2001).
[8] M. C. Rogge et al., Phys. Rev. B 72, 233402 (2005).
[9] S. Gustavsson et al., Phys. Rev. Lett. 96, 076605 (2006).
[10] T. Fujisawa et al., Science 312, 1634 (2006).
[11] J. M. Elzerman et al., Nature 430, 431 (2004).
[12] W. Lu et al., Nature 423, 422 (2003).
[13] R. Schleser et al., Appl. Phys. Lett 85, 2005 (2004).
[14] T. Fujisawa et al., Nature 419, 278 (2002).
[15] O. Naaman et al., Phys. Rev. Lett. 96, 100201 (2006); S. Gustavsson et al. (2006), cond-mat/0607192.
[16] S. Amasha et al., (2006), in preparation.
[17] G. Granger et al., Phys. Rev. B 72, 165309 (2005).
[18] M. Ciorga et al., Phys. Rev. B 61, R16315 (2000).
[19] L. D. Landau and E. M. Lifshitz, Quantum Mechanics (Butterworth-Heinemann, 2003).
[20] D. H. Cobden et al., Phys. Rev. Lett. 81, 681 (1998).
[21] J. C. Chen et al., Phys. Rev. B 74, 045321 (2006).
[22] L. P. Kouwenhoven et al., in Mesoscopic Electron Transport, edited by L. Sohn, L. Kouwenhoven, and G. Schon (Kluwer Academic Publishers, 1997), NATO ASI Series E 345, pp. 105{214.
[23] J. I. Climente et al., Phys. Rev. B 74, 035313 (2006).
[24] U. Bockelmann, Phys. Rev. B 50, 17271 (1994).